Rapid assembly dynamics of the *Escherichia coli* FtsZ-ring demonstrated by fluorescence recovery after photobleaching

Jesse Stricker*, Paul Maddox†, E. D. Salmon†, and Harold P. Erickson*‡

*Department of Cell Biology, Duke University Medical Center, Box 3709, Durham, NC 27710; and †Department of Biology, CB# 3280, University of North Carolina, Chapel Hill, NC 27599

Edited by J. Richard McIntosh, University of Colorado, Boulder, CO, and approved December 17, 2001 (received for review November 5, 2001)

FtsZ, the major cytoskeletal component of the bacterial cell-division machine, assembles into a ring (the Z-ring) that contracts at septation. FtsZ is a bacterial homolog of tubulin, with similar tertiary structure, GTP hydrolysis, and *in vitro* assembly. We used green fluorescent protein-labeled FtsZ and fluorescence recovery after photobleaching to show that the *E. coli* Z-ring is extremely dynamic, continually remodeling itself with a half-time of 30 s. ZipA, a membrane protein involved in cell division that colocalizes with FtsZ, was equally dynamic. The Z-ring of the mutant *ftsZ84*, which has 1/10 the guanosine triphosphatase activity of wild-type FtsZ *in vitro*, showed a 9-fold slower turnover *in vivo*. This finding implies that assembly dynamics are determined primarily by GTP hydrolysis. Despite the greatly reduced assembly dynamics, the *ftsZ84* cells divide with a normal cell-cycle time.

The processes involved in bacterial cell division are strikingly different from those involved in eukaryotic cytokinesis. Whereas animal cells use a contractile ring of actin and myosin, bacteria form a ring of FtsZ, a cell division protein found in almost every prokaryotic species. This ring, known as the Z-ring, is attached to the inner membrane and contracts during septation. FtsZ is the major protein in the ring, although other proteins necessary for division have been identified in *Escherichia coli* and other species (1–3). FtsZ is a homolog of tubulin: both proteins share very similar tertiary structures (4), hydrolyze GTP, and assemble into straight and curved protofilaments (5–8).

Although the substructure of the Z-ring is not known, *in vitro* studies suggest that it is based on protofilaments, perhaps associated into multistranded structures. FtsZ polymerizes into single protofilaments under many *in vitro* solution conditions. Under other conditions, the protofilaments associate side-by-side to form ribbons or sheets (5, 7, 9). An assembly mixture of single protofilaments hydrolyzes GTP at a rate of five molecules per min per FtsZ (10) in physiological buffer conditions (350 mM KCl, pH 7.5; ref. 11). There is no evidence that FtsZ undergoes dynamic microtubule-like instability. Instead, a model of isodesmic assembly has been proposed in which each GTP hydrolysis event results in fragmentation of the protofilament, followed by nucleotide exchange and reannealing (12). In this model, the guanosine triphosphatase (GTPase) activity would reflect very rapid fragmentation/reannealing dynamics, in which every subunit is turned over, in the sense of breaking and reforming an interface, five times per minute at steady-state.

In rapidly dividing *E. coli* cells, the Z-ring forms in the center of the cell about 1 to 5 min after division, remains for 15 min, and then quickly constricts to divide the cell (13–15). Although the Z-ring appears static when observed by fluorescence of FtsZ-gfp, it could be exchanging subunits with a cytoplasmic pool. In an attempt to directly investigate the assembly dynamics of FtsZ, we performed fluorescence recovery after photobleaching (FRAP) on Z-rings containing a small proportion of FtsZ-gfp.

Materials and Methods

Strains and Plasmids. MC1000 (16) was used as a wild-type strain. JFL101 [*ftsZ84*(ts), supplied by J. Lutkenhaus, University of Kansas Medical Center] (17) grows normally at 30°, but its Z-rings disassemble, and it grows into filaments at 42°. PB103(λCH50) (*zipA-gfp*, supplied by P. de Boer, Case Western Reserve University, Cleveland, OH) (18) carries a stable phage containing *zipA-gfp* under control of the *lac* promoter. LMG64 [*ftsI*(ts), supplied by D. S. Weiss, Harvard Medical School] (19), grows normally at 30°, but grows into filaments with multiple Z-rings at 42°.

pBZG is based on pBAD18 plasmid (20) and expresses a fusion protein consisting of *E. coli* FtsZ, an HIIH linker, mut2 green fluorescent protein (gfp), and a 6xHis C-terminal tag under the control of the pBAD promoter. The junctions of this plasmid were confirmed by sequencing. pBZ84G was derived from pBZG by mutating the *ftsZ* to *ftsZ84* (G105S) by using the QuickChange kit (Stratagene), following manufacturer's directions and confirming the mutation by sequencing.

Growth and Induction. All strains were grown in Mops+ medium (supplemented with amino acids, vitamins, and nucleic acids) as in ref. 21 to avoid the background fluorescence associated with casamino acids. Ampicillin was added to growth media for transformed strains at a concentration of 100 μg/ml. Either glucose or glycerol (0.2%) was added as a carbon source to repress or allow, respectively, expression of FtsZ-gfp. MC1000(pBZG) or LMG64(pBZG) were grown in Mops+ containing 0.2% glucose at 37°. For microscopy and FRAP, overnight cultures were diluted into Mops+ medium containing 0.2% glycerol and grown at 37° to A_{600} = 0.5, then induced by the addition of arabinose to 0.00005% and grown at 37° for 45 min before being transferred back into fresh Mops+ medium with glycerol and no arabinose (preventing further FtsZ-gfp expression) for viewing.

JFL101(pBZ84G) was grown in Mops+ containing 0.2% glucose at 30°. For microscopy and FRAP, overnight cultures were diluted into Mops+ containing 0.2% glycerol and 0.00001% arabinose and grown at 30° to A_{600} = 0.5 (approximately 15 h), then transferred to fresh Mops+ containing 0.2% glycerol and no arabinose for viewing. Induction in JFL101(pBZ84G) was less reproducible than induction in MC1000(pBZG), necessitating longer growth with lower concentrations of arabinose. The doubling time of JFL101(pBZ84G) did not change upon induction, and cells with normal Z-rings were common. PB103(λCH50) was grown and induced as in ref. 18.

Microscopy and FRAP. Image acquisition and FRAP measurements were performed on a Nikon TE300 fluorescence micro-

This paper was submitted directly (Track II) to the PNAS office.

Abbreviations: FRAP, fluorescence recovery after photobleaching; GTPase, guanosine triphosphatase; gfp, green fluorescent protein.

‡To whom reprint requests should be addressed. E-mail: h.erickson@cellbio.duke.edu.

The publication costs of this article were defrayed in part by page charge payment. This article must therefore be hereby marked "*advertisement*" in accordance with 18 U.S.C. §1734 solely to indicate this fact.

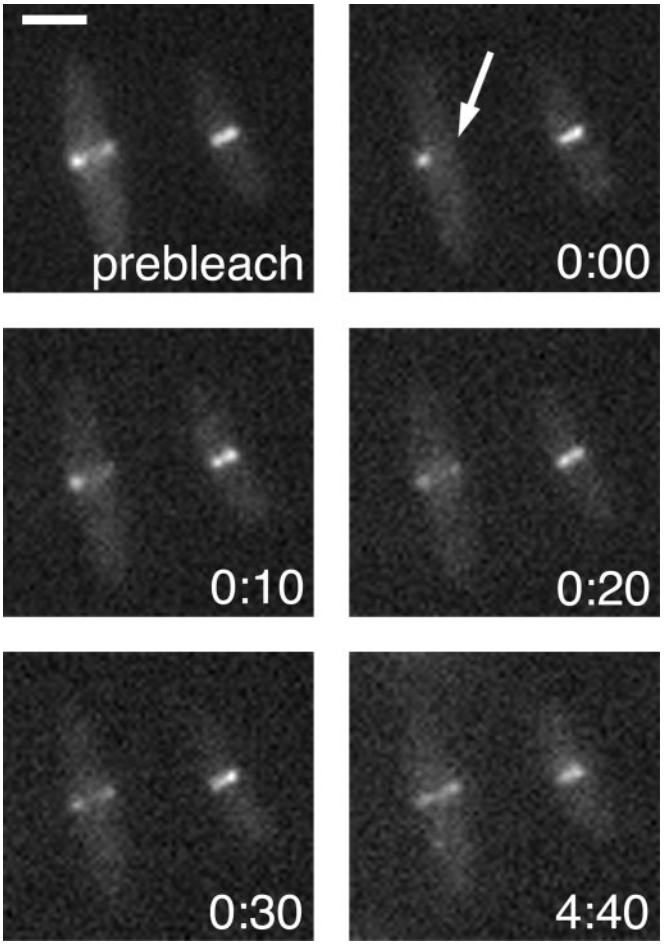

Fig. 1. FRAP analysis of FtsZ. MC1000(pBZG) cells were visualized on the microscope slide. Half of the Z-ring of the cell on the left was laser photobleached at the arrow, and recovery of fluorescence was monitored. Panels were photographed at times indicated (minutes:seconds). (Bar = 2 μm.)

scope system with a temperature-controlled stage as described (22). Briefly, cells were suspended in Mops+ medium with glycerol, attached to polylysine-coated coverslips, and then imaged through a 100×/1.4 numerical aperture Plan Apochromat objective lens with an Orca cooled charge-coupled device camera (Hamamatsu Photonics, Hamamatsu, Japan). All observations were performed at 30°C. Exposures were controlled by METAMORPH software (Universal Imaging, Media, PA). Photobleaching was achieved by focusing an argon ion laser to a diffraction-limited spot on the specimen for an exposure of ≈25 ms. Wide-field fluorescent images of the cells were acquired before and after photobleaching by custom time-lapse recording of digital images with 12-bit gray levels. Images of MC1000(pBZG) cells and PB103(λCH50) cells were obtained every 10–15 s for 2 min, after which the time-lapse interval was increased to 2 min. Images of JFL101(pBZ84G) cells were obtained with a time-lapse interval of 2–3 min. Measurements of integrated fluorescence in regions of the cell as well as calculation of the half-time and percent fluorescence recovery in the 0.5 μm wide photobleached region of rings were performed as described (22).

Results

E. coli MC1000 cells were transformed with pBZG, an inducible plasmid expressing FtsZ-gfp, and induced such that Z-rings were visible by fluorescence microscopy (Fig. 1 *Upper Left*). The morphology of these rings was similar to that of Z-rings visualized by immunofluorescence microscopy, and cell growth and division were unaffected. Western blot analysis showed that less than 25% of the total FtsZ in the cell was FtsZ-gfp (data not shown).

Analysis of the distribution of FtsZ-gfp in the cells by integrating fluorescence over the ring and the cytoplasm showed that only ≈30% of the FtsZ in the cell is incorporated into the Z-ring. The remainder of the FtsZ is diffused throughout the cell, presumably as free cytoplasmic subunits or small assemblies. This result means that at any given time, there is a large soluble pool of FtsZ available to exchange into the ring. It also means that the Z-ring is, on average, only six to seven protofilaments thick (see ref. 10 for this calculation), perhaps explaining why the Z-ring has never been seen by thin-section electron microscopy.

To investigate whether exchange occurs between the Z-ring and the cytoplasmic pool, we performed FRAP analysis on the gfp-labeled Z-rings. FRAP uses a focused laser beam to photobleach a portion of a fluorescent structure and measures the recovery of fluorescent signal in the photobleached area caused by exchange of subunits from outside of the photobleached area. Z-rings recovered fluorescence very quickly (Fig. 1), with a mean halftime of recovery of 31.7 ± 3.4 s (mean ± SE, n = 13) at 30°. Z-rings that were entirely photobleached did not fully recover fluorescence because of the lower pool of fluorescent subunits available after bleaching. However, Z-rings that had been only partially bleached usually recovered fluorescence to nearly prephotobleaching levels.

We also performed FRAP on LMG64(pBZG) cells (23), which are *ftsI*(ts) and cannot divide at the restrictive temperature but can still elongate. These cells contain multiple fluorescent Z-rings and a larger total pool of available FtsZ-gfp subunits. When a single Z-ring was repeatedly bleached, it recovered fully with the same ≈30 s half life as in the wild-type cells (data not shown).

After photobleaching, fluorescence always reappeared in structures identical to those seen before photobleaching, even in the case of rare aberrant FtsZ structures such as helices or punctate rings. To rule out the possibility that recovery of fluorescence was caused by recovery of gfp fluorophores, we fixed cells with 4% (wt/vol) paraformaldehyde and measured their FRAP recovery rate. The Z-rings appeared normal but showed no recovery of fluorescence into the photobleached area, whether at the Z-ring or in the cytoplasm, after 20 min (data not shown). This result demonstrates that recovery of fluorescence depended on exchange of fluorescent FtsZ subunits from the cytoplasmic pool. The photobleaching procedure was not harmful to the cells or the rings; completely photobleached cells grew and divided on the slide in a manner similar to that of adjacent unbleached cells (data not shown).

We considered the possibility that the dynamic behavior of the Z-ring is required for its initial assembly and localization, but that during constriction, the Z-ring becomes a stable scaffold for a force-generating mechanism. However, we found no relationship between cell length (used as a marker for progress into the cell cycle in the logarithmic phase cells being analyzed) and halftime of recovery (data not shown). FRAP analysis of cells with visible division furrows (Fig. 2) showed a halftime of recovery of 35.6 ± 14.2 s (mean ± SE, n = 10). This rate of recovery is similar to that of nondividing cells, indicating that the Z-ring is dynamic during constriction. Intriguingly, some dividing cells had ≈60% of their FtsZ incorporated into the Z-ring, twice the proportion in the Z-ring of nondividing cells; however, this increase in incorporation into the Z-ring was not consistently observed.

The dynamics and exchange of subunits in the microtubule cytoskeleton are coupled to GTP hydrolysis. FtsZ hydrolyzes GTP at a rate of 5 min^{-1} *in vitro* (10), a rate similar to the

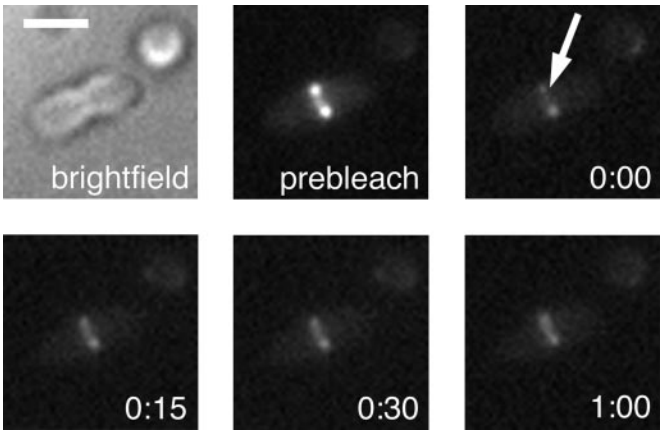

Fig. 2. FRAP analysis of the Z-ring in a dividing cell. (*Upper Left*) Brightfield image of an MC1000(pBZG) cell in the process of division. The cell was photobleached at the arrow and the recovery of fluorescence was monitored. Panels were photographed at times indicated (minutes:seconds). (Bar = 2 μm.)

exchange *in vivo*. We tested the possible coupling of FtsZ exchange to GTP hydrolysis with an *E. coli* strain (JFL101) that has the mutant *ftsZ84* allele at the genomic locus (17). This mutant FtsZ has ≈10% of the GTPase activity of wild-type FtsZ when measured *in vitro* (24, 25). Despite this greatly reduced GTPase, cells carrying *ftsZ84* seem to divide normally at 30°, with the same cell-cycle timing as wild-type cells. We inserted the *ftsZ84* mutation (G105S) into our *ftsZ-gfp* plasmid to create pBZ84G and transformed JFL101 cells with this mutated plasmid. Thus, both the genomic and the gfp-labeled FtsZ carried the *ftsZ84* mutation. Although FtsZ84-gfp induction in JFL101(pBZ84G) was less reproducible, we found conditions in which many of the cells contained a single bright medial ring of normal appearance, and we performed FRAP analysis on these rings.

Quantitative fluorescence analysis showed that in these *ftsZ84* cells, the Z-rings contained ≈65% of the FtsZ in the cell, a proportion twice as high as that found for wild-type FtsZ. In our FRAP studies, Z-rings consisting of FtsZ84 recovered much more slowly than wild-type Z-rings (Fig. 3 and Fig. 4). The halftime of recovery was 284.0 ± 19.5 s (mean ± SE, $n = 12$) at 30°C, ≈9-fold longer than that of wild-type rings. This finding corresponds very closely to the difference in *in vitro* GTPase rate and suggests that the turnover of FtsZ *in vivo* is tightly coupled to GTP hydrolysis. This fact may also explain the high proportion of FtsZ84 associated with the ring. If turnover and release from the ring are coupled to GTP hydrolysis, but incorporation into the ring is not, then FtsZ that has a slower rate of hydrolysis might accumulate in the ring.

In *E. coli*, the transmembrane protein ZipA, an essential component of the division machinery, binds FtsZ and may serve as a membrane tether (18). If the ZipA ring were stable, then it might act as a scaffold for FtsZ accumulation. Even if it were connected to the Z-ring only through its attachment to FtsZ, its turnover and exchange might be slowed because it is confined to the membrane. We used a *zipA-gfp* strain, PB103(λCH50), to determine the assembly dynamics of ZipA in the Z-ring. Approximately 30% of the ZipA in the cell was incorporated into a medial ring, a proportion similar to that seen with FtsZ. The ZipA ring appeared to be as dynamic as FtsZ (Fig. 5), with a recovery halftime of 27.9 ± 6.0 s (mean ± SE, $n = 9$). It is possible that the entire division machinery undergoes a similar dynamic exchange.

Discussion

The quick recovery of fluorescence that we observe implies that the Z-ring is an extremely dynamic structure, continually exchanging subunits with a cytoplasmic pool. The halftime of recovery seen with FtsZ is roughly comparable to the most dynamic cytoskeletal structures. Spindle microtubule arrays show a halftime of recovery of ≈10–20 s (26, 27), whereas other, more stable structures recover much more slowly; such structures include interphase microtubule arrays, halftime of recovery of 200 s (27), actin stress fibers, halftime of recovery of 500 s (28), or vimentin, halftime of recovery of 10–15 min (29). Yeast metaphase mitotic spindles show a halftime of recovery of ≈1 min, similar to that seen here (22).

Two previous studies have already demonstrated rapid dynamics of assembly during the periods of active assembly or disassembly of the Z-ring. Sun and Margolin (14) found that FtsZ rings assembled in daughter cells very soon after the parental Z-ring constricted and disassembled. Significantly, it took only ≈1–3 min for the new rings to go from very dim to full brightness. Our work now extends this picture of rapid initial assembly to show that once the ring has reached its steady-state,

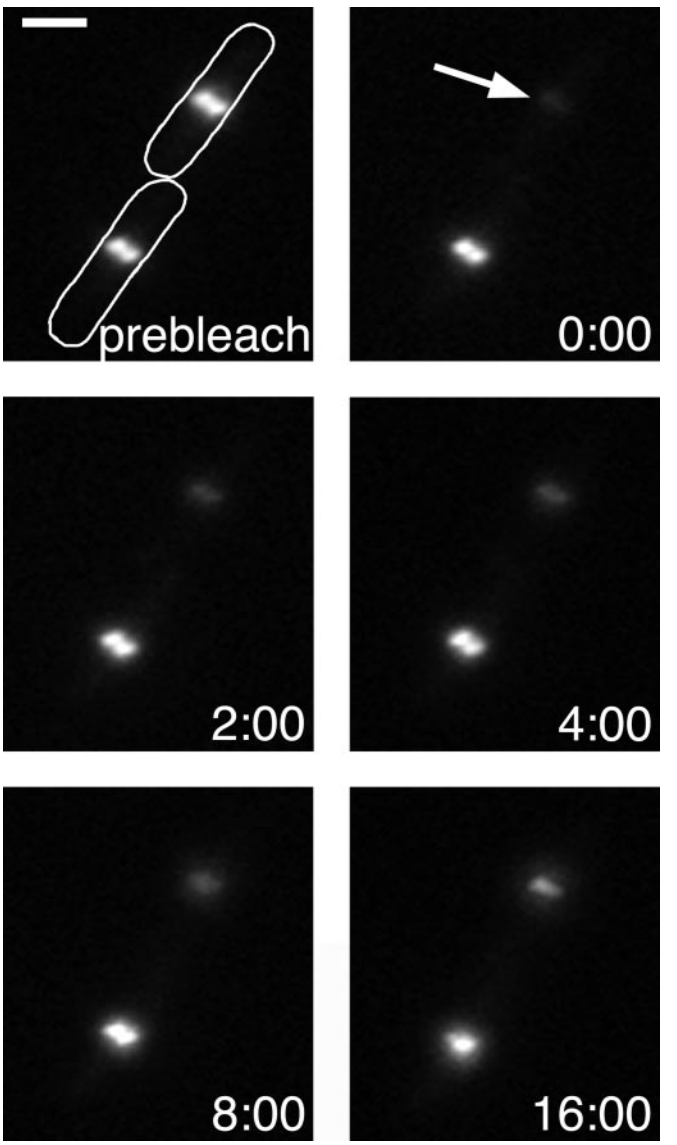

Fig. 3. FRAP analysis of FtsZ84. JFL101(pBZ84G) cells were visualized on the microscope slide. Two cells are outlined in *Upper Left*. The entire Z-ring of the cell at *Upper Right* was laser photobleached as indicated by the arrow, and recovery of fluorescence was monitored over time. Panels were photobleached at times indicated (minutes:seconds). (Bar = 2 μm.)

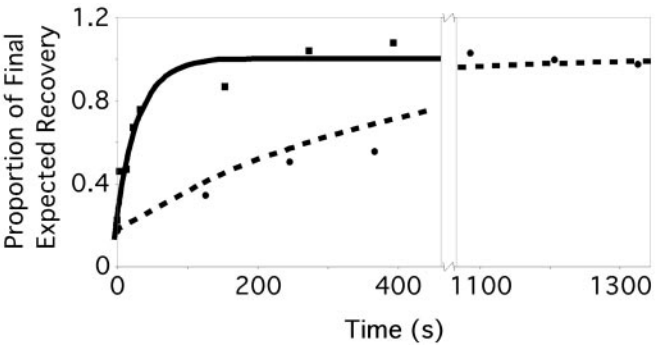

Fig. 4. Comparison of recovery of fluorescence of wild-type FtsZ and FtsZ84. Data point values are normalized to the expected final recovery of each species of FtsZ, determined by assuming an exponential recovery with the halftimes given in the text and taking into account the initial loss of fluorophores caused by photobleaching. Note the discontinuous *x* axis. Filled circles represent time points for the MC1000(pBZG) cell shown in Fig. 1; filled squares represent the JFL101(pBZ84G) cell shown in Fig. 2*A*. The curves indicate theoretical recoveries, given the halftimes of recovery in the text, normalized to final expected recovery as for the experimental data points. The solid curve represents wild-type FtsZ, and the dashed curve represents FtsZ84.

it continues to exchange subunits and remodel at least as fast as the initial assembly. Presumably, this exchange also occurs as the ring is initially assembled. In the second study, Addinall *et al.* (30) found that Z-rings of FtsZ84 disassembled completely in 1 min when shifted to 42°C, which is much faster than the ≈5 min half time for remodeling we observed at 30°C. Below, we suggest that remodeling within the ring may be much faster than exchange with the cytoplasmic pool, so this rapid disassembly may indicate the total rate of fragmentation when reannealing is blocked. When shifted from 42° back to 30°C, the Z-rings reassembled over a period of 5 min, which is similar to the remodeling rate we observed.

In any study using gfp-labeled proteins, it is possible that labeled protein may behave differently from unlabeled. Previous studies have concluded that FtsZ-gfp coassembles with the endogenous FtsZ to label the Z-ring, is at least partially functional, and causes no aberrations when expressed at less than 30% of the normal level (13, 14). It is possible that a decreased activity of FtsZ-gfp is the reason that only 30% of FtsZ-gfp was in the Z-ring. However, the fact that 65% of FtsZ84-gfp localizes to the Z-ring suggests that this is not the case. Although it is difficult to prove conclusively, we think it is likely that the localization and dynamics of FtsZ-gfp reflect that of the native FtsZ.

If FtsZ *in vivo* is hydrolyzing GTP at the rate of five molecules per min per FtsZ (the rate measured *in vitro* for physiological conditions; ref. 10), the 15,000 molecules in an average *E. coli* cell would be consuming 1,250 molecules of GTP per s. This hydrolysis may seem to be a significant energetic burden to recycle subunits into the Z-ring, but it is actually an insignificant fraction of the cell's metabolism. Actively growing *E. coli* have been measured to consume 6.2×10^6 molecules of O_2 per s, which would produce 3.7×10^7 high-energy phosphates per s (calculated assuming three phosphates per oxygen atom; ref. 31). Thus, the five GTPs hydrolyzed per min per FtsZ represent only 1/30,000 of the active cell's metabolism.

Although little is known about the structure and assembly of the Z-ring *in vivo*, much has been learned about FtsZ polymers from *in vitro* assembly studies. Depending on assembly conditions, FtsZ can assemble into single protofilaments or small bundles and sheets of protofilaments. If FtsZ assembly is cooperative, like microtubules, one would postulate an association of FtsZ subunits onto the ends of multifilament bundles. In contrast

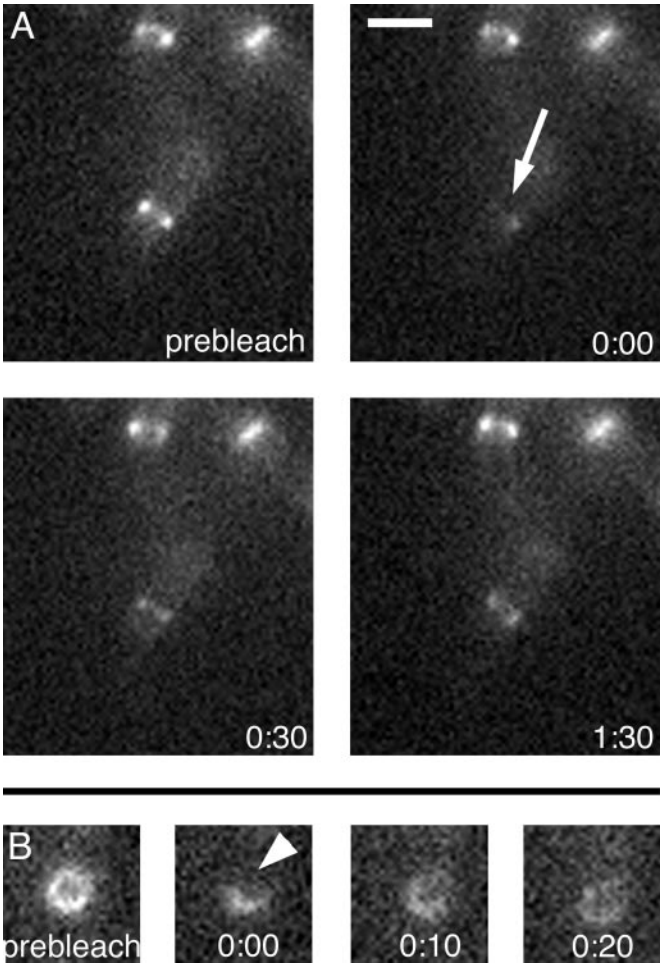

Fig. 5. FRAP analysis of ZipA. (*A*) PB103(λCH50) cells were laser photobleached at the ZipA ring (arrow); recovery of fluorescence was monitored over time. (*B*) A PB103(λCH50) cell was attached to the coverslip at its end, allowing a face view of the ZipA ring. This cell was photobleached at the arrowhead, and recovery of fluorescence was monitored. Fluorescence recovery appeared to take place at uneven rates around the circumference of this cell. All panels were photographed at times indicated (minutes:seconds). (Bar = 2 μm.)

to this, Romberg *et al.* (12) have described a theory of isodesmic assembly in which FtsZ subunits assemble into protofilaments one subunit wide. Assembly can occur by addition of single subunits or by annealing of filaments, and fragmentation can occur at any binding interface. In this model, all subunits in a protofilament are postulated to have bound GTP, and hydrolysis to GDP results in rapid fragmentation at that interface. The filament is able to reanneal after exchange of GDP for GTP. If the Z-ring is constructed from these isodesmic protofilaments, then we would expect to see a correlation between the GTPase activity of FtsZ and Z-ring stability.

Fig. 6 presents two models for FtsZ distribution in the bacterium and Z-ring structure. The top model is based on cooperative assembly. Protofilament bundles are localized to the Z-ring, and FtsZ in the cytoplasm is monomeric. The rapid dynamics of the ring would be explained best by a mechanism similar to dynamic instability, in which whole segments of the polymers disassemble into monomers and are replaced by new segments assembled from monomers. The bottom model is based on the isodesmic assembly hypothesis. At the 11 μM concentration of FtsZ obtained *in vivo* (10), the model predicts that virtually all of the FtsZ in the cell will be assembled into

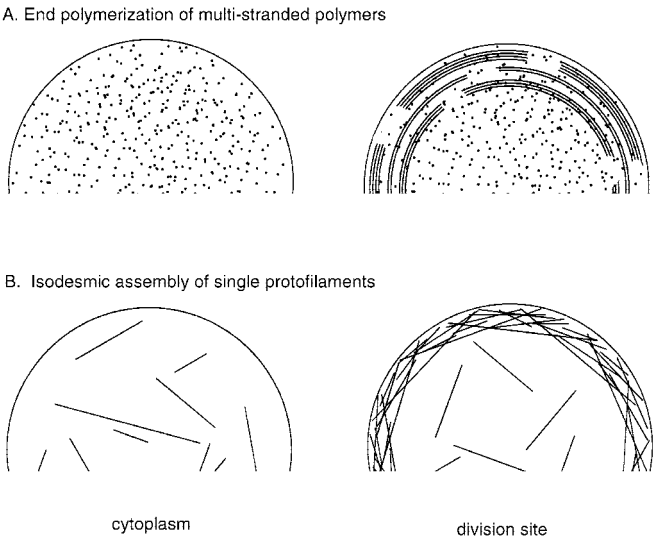

Fig. 6. Two models of how FtsZ protofilaments might be distributed in the Z-ring and cytoplasm. The semicircles are transverse cross sections of 200-nm thickness through the bacterium at the cytoplasm (*Left*) or Z-ring (*Right*), and the total number of subunits or protofilaments in this cell volume are shown. (*A*) A cooperative assembly model in which the Z-ring comprises multifilament bundles, and the cytoplasmic FtsZ is monomeric. In this model, assembly dynamics are thought to involve monomers exchanging onto the ends of the polymers. (*B*) An isodesmic assembly model. Protofilaments of length 40, 80, and 160 subunits are used to indicate the distribution of lengths around the mean of 80 subunits. In this model, the cytoplasmic FtsZ is largely assembled into protofilaments, and remodeling involves exchanging fragments of protofilaments between the cytoplasm and Z-ring. Attachments of protofilaments to each other and/or to the membrane are not shown but must occur in either model. The models are not exclusive of each other, as assembly could begin with single filaments, which are clustered into multistranded polymers in the Z-ring.

protofilaments with an average length of ≈80 subunits (protofilaments averaging 25 subunits have been observed *in vitro* at a 10-fold lower FtsZ concentration; ref. 12). This model suggests that the pool of cytoplasmic FtsZ may consist of protofilaments rather than single subunits. A quantity of 15,000 molecules of FtsZ would give ≈180 protofilaments of 80 subunits. (More precisely, there would be a distribution around this length.) Thirty percent, or ≈56 protofilaments, would be concentrated in the Z-ring, with the remainder distributed throughout the cytoplasm. In this model, the assembly dynamics of the Z-ring would involve the exchange of short pieces of protofilaments, released after GTP hydrolysis and fragmentation, rather than of single subunits. In either model, there are likely to be events during which FtsZ is released from the Z-ring but reassociates within the ring, rather than diffusing to the cytoplasm. These internal remodeling events are likely to exceed those resulting in net exchange, which implies that the total assembly dynamics of the Z-ring are faster than the exchange measured by FRAP.

The isodesmic assembly model also postulates a pathway for protofilament fragmentation that is independent of GTP hydrolysis. In the model developed from *in vitro* studies (12), this event would occur at a rate of 0.9 per min. However, the comparative dynamics of wild-type FtsZ and FtsZ84 suggest that the dynamics of the Z-ring are dominated by the GTPase-dependent mechanism, and that the hydrolysis-independent pathway does not play a major role in subunit turnover.

The remarkably dynamic nature of the Z-ring at first seems enigmatic either for its role as a scaffold or for generating a constriction force. In eukaryotes, the actin filaments provide a stable scaffold upon which myosin motors operate to generate the force of constriction. Whatever the mechanism for force generation in the Z-ring, it must be able to operate with the constant turnover of its scaffold. But we also should consider the possibility that the rapid turnover may be more than an obstacle for force generation. Fragmentation and annealing might be part of the mechanism for generating the force for constriction. For example, if a mechanism existed for sequestering FtsZ in the cytoplasm at the time of constriction, protofilament pieces might be removed from the ring more quickly than they are replaced. Reannealing of the remaining filaments could only occur when they move closer together, and this might lead to a circumferential constriction that could power cell division.

We would like to thank Tom Melby for construction of pBZG and Dr. Petra Levin and Dr. Laura Romberg for helpful comments on the manuscript. This study was funded by National Institutes of Health Grants GM28553 (to H.P.E.) and GM60678 (to E.D.S.).

1. Bramhill, D. (1997) *Annu. Rev. Cell Dev. Biol.* **13,** 395–424.
2. Lutkenhaus, J. & Addinall, S. G. (1997) *Annu. Rev. Biochem.* **66,** 93–116.
3. Rothfield, L., Justice, S. & Garcia-Lara, J. (1999) *Annu. Rev. Genet.* **33,** 423–448.
4. Löwe, J. (1998) *J. Struct. Biol.* **124,** 235–243.
5. Erickson, H. P., Taylor, D. W., Taylor, K. A. & Bramhill, D. (1996) *Proc. Natl. Acad. Sci. USA* **93,** 519–523.
6. Lu, C. L., Reedy, M. & Erickson, H. P. (2000) *J. Bacteriol.* **182,** 164–170.
7. Löwe, J. & Amos, L. A. (1999) *EMBO J.* **18,** 2364–2371.
8. Löwe, J. & Amos, L. A. (2000) *Biol. Chem.* **381,** 993–999.
9. Yu, X. C. & Margolin, W. (1997) *EMBO J.* **16,** 5455–5463.
10. Lu, C., Stricker, J. & Erickson, H. P. (1998) *Cell Motil. Cytoskeleton* **40,** 71–86.
11. Cayley, S., Lewis, B. A., Guttman, H. J. & Record, M. T., Jr. (1991) *J. Mol. Biol.* **222,** 281–300.
12. Romberg, L., Simon, M. & Erickson, H. P. (2001) *J. Biol. Chem.* **276,** 11743–11753.
13. Ma, X., Ehrhardt, D. W. & Margolin, W. (1996) *Proc. Natl. Acad. Sci. USA* **93,** 12998–13003.
14. Sun, Q. & Margolin, W. (1998) *J. Bacteriol.* **180,** 2050–2056.
15. Den Blaauwen, T., Buddelmeijer, N., Aarsman, M. E., Hameete, C. M. & Nanninga, N. (1999) *J. Bacteriol.* **181,** 5167–5175.
16. Casadaban, M. J. & Cohen, S. N. (1980) *J. Mol. Biol.* **138,** 179–207.
17. Lutkenhaus, J., Wolf-Watz, H. & Donachie, W. D. (1980) *J. Bacteriol.* **142,** 615–620.
18. Hale, C. A. & De Boer, P. A. J. (1997) *Cell* **88,** 175–185.
19. Guzman, L. M., Weiss, D. S. & Beckwith, J. (1997) *J. Bacteriol.* **179,** 5094–5103.
20. Guzman, L. M., Belin, D., Carson, M. J. & Beckwith, J. (1995) *J. Bacteriol.* **177,** 4121–4130.
21. Neidhardt, F. C., Bloch, P. L. & Smith, D. F. (1974) *J. Bacteriol.* **119,** 736–747.
22. Maddox, P. S., Bloom, K. S. & Salmon, E. D. (2000) *Nat. Cell Biol.* **2,** 36–41.
23. Weiss, D. S., Pogliano, K., Carson, M., Guzman, L. M., Fraipont, C., Nguyen-Distèche, M., Losick, R. & Beckwith, J. (1997) *Mol. Microbiol.* **25,** 671–681.
24. RayChaudhuri, D. & Park, J. T. (1992) *Nature (London)* **359,** 251–254.
25. de Boer, P., Crossley, R. & Rothfield, L. (1992) *Nature (London)* **359,** 254–256.
26. Salmon, E. D., Leslie, R. J., Saxton, W. M., Karow, M. L. & McIntosh, J. R. (1984) *J. Cell Biol.* **99,** 2165–2174.
27. Saxton, W. M., Stemple, D. L., Leslie, R. J., Salmon, E. D., Zavortink, M. & McIntosh, J. R. (1984) *J. Cell Biol.* **99,** 2175–2186.
28. Wang, Y. L. (1987) *J. Cell Biol.* **105,** 2811–2816.
29. Vikstrom, K. L., Lim, S.-S., Goldman, R. D. & Borisy, G. G. (1992) *J. Cell Biol.* **118,** 121–129.
30. Addinall, S. G., Cao, C. & Lutkenhaus, J. (1997) *J. Bacteriol.* **179,** 4277–4284.
31. Imlay, J. A. & Fridovich, I. (1991) *J. Biol. Chem.* **266,** 6957–6965.